CLIMA 2016 - proceedings of the 12th REHVA World Congress

volume 9

Heiselberg, Per Kvols

Publication date:
2016

Document Version
Publisher's PDF, also known as Version of record

Link to publication from Aalborg University

Citation for published version (APA):
Heiselberg, P. K. (Ed.) (2016). *CLIMA 2016 - proceedings of the 12th REHVA World Congress: volume 9*. Department of Civil Engineering, Aalborg University.

Heat transfer enhancement of free convection flows in vertical 2D-channels with Kármán vortex streets – an experimental study

Paul Mathis[#1], Tobias Maria Burgholz[#], Henning Freitag[#], Max Rohn[#], Markus Hans Schraven[#], Dirk Müller[#]

[#]E.ON Energy Research Center, Institute for Energy Efficient Buildings and Indoor Climate, RWTH Aachen University
Mathieustr. 10, 52074 Aachen, Germany

[1]pmathis@eonerc.rwth-aachen.de

Abstract

This paper presents an experimental study of heat transfer enhancement in free convection channel flows. The flow in a vertical two-dimensional channel with heated walls is modified through circular cylinders of different diameters and installation heights. A vortex street is triggered downstream, leading to strong convective mixing of the fluid, bringing cooler fluid from the central part of the channel to the heated walls and thus increasing the heat transfer significantly. Heat transfer enhancements of up to 41.9% are found with a circular 2D-cylinder with a blockage ratio of 0.45. The dependency of heat transfer enhancement on different blockage ratios and installation heights is presented. The heat transfer enhancement is achieved without additional energy effort for propelling the fluid, as the flow is purely driven by natural convection. Visualizations of the flow and PIV measurement data is shown, indicating a three-dimensional flow structure in the reference case without a cylinder as well as in the cylinder cases – despite the two-dimensional geometry.

Keywords - heat transfer enhancement, free convection flow, vortex street, vortex promoters

1. Introduction

Heat transfer by natural convection in vertical channels has an important impact on the performance of different HVAC systems. Typical heat radiators, for instance, deliver approximately two thirds of their heating performance via convector channels. As the flow in the channel is assumed to be laminar, the main heat transfer mechanism from wall to fluid is conduction and the temperature boundary layer is comparatively small. Consequently, the temperature gradient and hence the heat transfer between wall and fluid is low. Enhancing the heat transfer in such channels yields a significant improvement in performance.

A simulative investigation of purely natural convection flows in vertical channels has been conducted by Mathis et al. [1], revealing a great potential of increasing the heat transfer from the walls to the fluid by placing a vortex promoter into the flow path and by that triggering a Kármán vortex street. The vortices separating from blunt bodies cause convective mixing of the flow, bringing cooler fluid from the center of the channel to the heated walls, thus increasing the temperature gradient and by that the heat transfer. The previously conducted study by Mathis et al. indicates a high potential of heat transfer enhancement in vertical channels compared to the reference setup without vortex promoter. This suggests that exploiting the positive impact of Kármán vortices on the heat transfer might increase the specific heat performance of heat exchangers operated by natural convection drastically. So far, mainly heat transfer from heated blunt bodies in forced and mixed convection channel flows are addressed in the literature ([4], [8], [8], [10], [12], [13]). Heat transfer enhancement (HTE) through vortex promoters in heated channels is limited to forced convection only, indicating a high potential but at high cost in terms of pressure drop ([1], [2], [5], [8]).

In this study, an experimental investigation of the heat transfer enhancement in vertical 2D-channels is presented. It is analyzed how blockage ratio and channel height of different cylinders impact the heat performance.

2. Methods

2.1 Heat delivery measurements

Test facility: All measurements are conducted with a uniform channel wall temperature and in a temperature-controlled climate chamber. The vertical channel is 640 mm high, 42 mm wide and has a depth of 470 mm (Figure 1). As the depth of the channel is considerably greater than its width, the flow is assumed to be two-dimensional. The inlet is well-rounded (r = 95 mm) and therefore laminar and smooth upstream flow conditions are provided. By separately tempering the enclosing surfaces of the climate chamber (walls, ceiling and floor), an inlet air temperature of $T_{inlet} \approx 19.4$ °C is obtained.

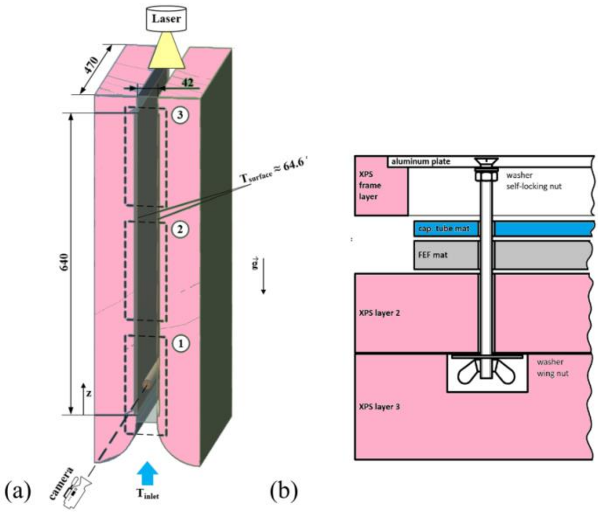

Figure 1: (a) Geometry of the channel flow PIV-setup; (b) schematic illustration of the different layers.

The heat is delivered to the walls with synthetic capillary tube mats that are embedded in XPS insulation (Figure 1). An aluminum plate delivers the heat from the capillary mats to the channel. As the thermal connection between the capillary tube mats and the aluminum plate is a key prerequisite for a uniform surface temperature, thermal heat sink paste is applied on the inner contact surface between plate and capillary tube mat. To prevent recirculation areas within the channel the aluminum plate is integrated into the insulation frame in such a way that a smooth wall without any protrusions is guaranteed. The plate thickness of 3 mm represents a compromise between a high thermal conductivity coefficient of 237 W/(m K) for aluminum [14] in order to ensure a uniform wall temperature and a system with relatively low thermal inertia.

Experimental setup and procedure: An external supply unit provides the test facility with a constant volumetric flow of $\dot{V}_{water} = 1.02$ l/min. Supply and return temperature of the water vary as T_{supply} is constantly adjusted by a PID controller to keep the central surface temperature $T_{surface}$ at about 64.6 °C at all times. $T_{surface}$ is measured by a Pt100 temperature sensor that is installed halfway up the heated wall (Figure 1).

The emitted heat is calculated according to equation (1):

$$\dot{Q} = \rho_{water}\, \dot{V}_{water}\, c_{P,water} \left(T_{supply} - T_{return}\right) \\ = \dot{m}_{air}\, c_{P,air} \left(T_{inlet} - T_{outlet}\right) \tag{1}$$

Both specific heat capacity and density of water are given for $T_{ref} = 70$ °C and amount to $c_{Pwater} = 4190$ J/(kg K) [2] and $\rho_{water} = 0.978$ kg/m³ [15], respectively. All measurement values are time-averaged over periods of 60 min each.

Before the impact of different cylinders and channel heights on the heat transfer can be examined, the idle heat output $\dot{Q}_{idle}$ of the test facility is measured and calculated according to equation (1). $\dot{Q}_{idle}$ is the heat loss of the test facility due to limited insulation. It is measured by suppressing the convective airflow, so that only the heat loss to the ambience is recorded. To determine the effectively emitted heat of the heated walls only, this heat loss is subtracted from all measured heat outputs. This approach enables a correct quantification of the heat transfer induced by the vortex street:

$$\dot{Q}_{eff} = \dot{Q}_{measured} - \dot{Q}_{idle} \tag{2}$$

All cylinder configurations are compared to a reference measurement without any cylinder in the channel. With the reference measurement completed, different cylinders (16, 19 and 25 mm diameter) are installed into the channel, each one at different heights (z = 0, 40, 80, 120, 160, 200, 240, 300, 400 and 500 mm). Channel heights refer to the lower edge of the aluminum plate (Figure 1). The heat transfer enhancement (HTE) is defined as the ratio between the difference in heat outputs and the effective reference heat output:

$$\mathrm{HTE} = \frac{\Delta\dot{Q}}{\dot{Q}_{eff,ref}} = \frac{\dot{Q}_{eff} - \dot{Q}_{eff,ref}}{\dot{Q}_{eff,ref}} = \frac{\dot{Q} - \dot{Q}_{idle} - (\dot{Q}_{ref} - \dot{Q}_{idle})}{\dot{Q}_{eff,ref}} = \frac{\dot{Q} - \dot{Q}_{ref}}{\dot{Q}_{eff,ref}} \tag{3}$$

2.2 Visualisation of the flow

To allow for optical investigation and thermal imaging, matte black coating with a particularly low degree of reflection is applied to all surfaces within the channel. From downstream of the inlet section, stage smoke is injected into the channel and illuminated by several light sheets. Photographs are then taken perpendicular to the channel through an acrylic glass sheet and from above the channel (Figure 1).

2.3 PIV measurements

Particle Image Velocimetry (PIV) is an optical and nonintrusive method for velocity measurements in fluid flows. Small tracer particles are added to the fluid and illuminated at the investigated area by a double-pulse laser light sheet. The particles scatter the light within the illuminated plane, which is simultaneously recorded by high quality cameras. Between the two light pulses, a displacement of the particles synchronously to the streaming fluid is recorded. By using correlation methods, the instantaneous velocity vectors are determined from the displacement and the time between the two pulses [17].

The applied system is a Dantec Dynamics system with a Nd:YAG Laser. Its two cavities allow producing laser pulses with a frequency of 15 Hz and a wavelength of 532 nm. The scattered light is recorded by a HiSense Neo camera, working with sCMOS technology and a recording speed of 50 fps. The necessary cooling is provided by water, as the usual air cooling would impact the surrounding flow field and absorb the seeding particles. The seeding particles consist of Di-Ethyl-Hexyl-Sebacat (DEHS) and are small enough to not affect the flow, but big enough to scatter a sufficient amount of light. To provide reproducible and constant ambient conditions, the PIV measurements are performed in the temperature-controlled climate chamber with an ambient inlet air temperature of $\mathrm{T}_{\mathrm{inlet}} = 20°\mathrm{C}$.

The data is aquired in a two-dimensional, two component (2D2C) setup, where the laser is placed above the outlet working with a frequency of 13 Hz, leading to a plane perpendicular to the heated vertical walls (Figure 1). The camera is placed orthogonally to the laser plane. An unavoidable disadvantage of this constellation is the shadow below the introduced vortex promoters, prohibiting velocity measurements in this area. Since the laser plane can only be focussed on a certain length, the heated channel is divided into three overlapping sections (section 1, 2 and 3 in Figure 1). The data presented is a composition of the three sections.

3. Results and Discussion

3.1 Heat delivery measurements

The air in the vicinity of the heated walls is heated up, which results in a decline of air density, leading to buoyancy forces. This causes a natural convective flow. As the inlet velocity of the airflow is sufficiently small and the inlets are well-rounded, the flow enters the channel laminar and without causing considerable mixing. A stable temperature layer develops and in the airflow, conduction is the predominant heat transfer mechanism.

By inserting a blunt body like a cylinder into the channel flow, a Kármán vortex street is triggered, as the flow is in the region of laminar vortex streets with turbulent transition in the wake ([5], [15]). The Kármán vortices cause mixing of the colder inner fluid layer and the warmer peripheral boundary layers at the heated channel walls. The boundary layer decreases in size. Consequently, the wall temperature gradient and by that the local heat transfer coefficient increase.

The heat transfer enhancement caused by cylinders with diameters of 16, 19 and 25 mm (corresponding to blockage ratios of 0.38, 0.45 and 0.60) is presented in Figure 2. It is plotted for different blockage ratios over the channel height.

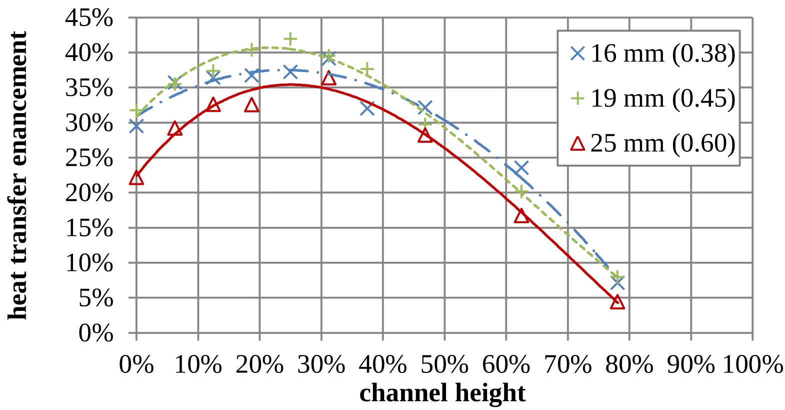

Figure 2: Heat transfer enhancement of different cylinder diameters at various channel heights

The maximum HTE of 41.9% is achieved for the 19 mm cylinder at a channel height of 25%. Also, the maximum values for the other cylinder diameters are found in the region of 20% to 30% of the channel height, however achieving slightly lower maximum HTE: 39.2% for the 16 mm cylinder and 36.4% for the 25 mm cylinder, both for a channel height of 31%.

The overall trend of the curves can be explained by the overlapping of three different effects: the leading edge effect at the beginning of the heated channel, the convective mixing by the vortex street and the additional flow resistance by the cylinder. When the cold fluid first enters the channel, the temperature difference between fluid and wall is maximum, leading to a high heat transfer [18]. Inserting a cylinder in the leading edge region does not increase the heat transfer that much, as the boundary layers are relatively small anyway. When inserting the cylinder further downstream, the boundary layers have grown in thickness and thus, the vortices shed by the cylinder disturb the boundary layers more effectively, leading to increased heat transfer. Adding the aspect of flow resistance (pressure drop), the decreasing trend further downstream the channel can be explained: as the vortices decrease in the wake of the cylinder, the convective mixing with its positive effect on the heat transfer and by that increasing buoyancy forces driving the flow, also decreases. When the cylinder is mounted further downstream, a smaller amount of the vortex street is situated in the channel, leading to a smaller amount of convective mixing. Consequently, the pressure drop by the cylinder is compensated less by the vortex street, leading to a decline of the overall heat transfer. This phenomenon is described in detail by Mathis et. al. in [1].

There is a dependency of HTE with regard to the blockage ratio of the channel: maximum HTE are achieved for a blockage ratio of 0.45 in this two-dimensional channel, larger and smaller blockage ratios yielding smaller HTE in the region of maximum HTE. However, with the investigation of cylinders with merely three different diameters, the data basis of this study is insufficient to determine an exact relation between blockage ratio and heat transfer enhancement. To allow for a more educated statement, further measurements with different diameters at a constant channel height should be conducted.

3.2 Visualisation of the flow

Figure 3 shows photographs of different configurations, taken perpendicular to the flow direction (sketch in Figure 1). In the configuration depicted in Figure 3 (a), no vortex promoter is installed. In the first half, the flow appears to be rather laminar while further downstream, it becomes more irregular.

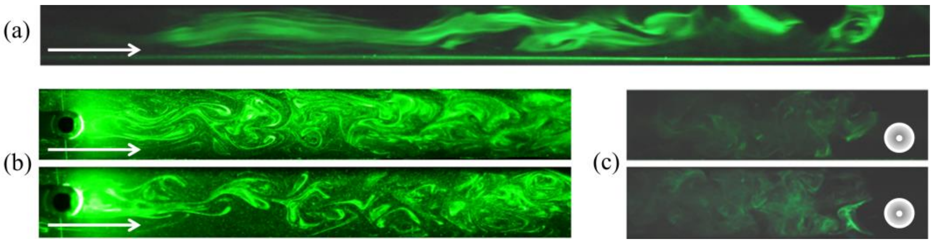

Figure 3: Flow visualization perpendicular to the channel. (a) no vortex promoter; (b) 19 mm cylinder at z = 80 mm at different time steps; (c) 19 mm cylinder at z = 80 mm from above the channel at different time steps

The next two photographs (b) show close-ups of a 19 mm cylinder at z = 80 mm, taken at different time steps. At the level of the cylinder, vortices of the Kármán vortex street occur that, however, do not alternate regularly and lack a well-defined structure as they advance downstream. Moreover, the recordings (c) show the outlet section and were taken from above, perpendicular to the cylinder axis, with the flow direction coming out of the paper plane. A three-dimensional vortex structure appears spreading unsteadily both in space and time, although the geometry is two-dimensional.

3.3 PIV measurements

In Figure 4, the instantaneous velocity distribution for the reference case and different blockage ratios is shown. In Figure 5, the averaged velocity fields over 300 data samples (i.e. 300/13 Hz = 23 s real time) for the same configurations are shown.

In the reference case, asymmetrical and time dependent flow structures are observed (Figure 4, top), although the averaged velocity field suggests a symmetrical distribution (Figure 5, top). This observation of three-dimensional structures corresponds to Figure 3 (a). Buoyant flows appear to lack symmetrical behavior in general, although the geometrical and inflow conditions might be symmetrical.

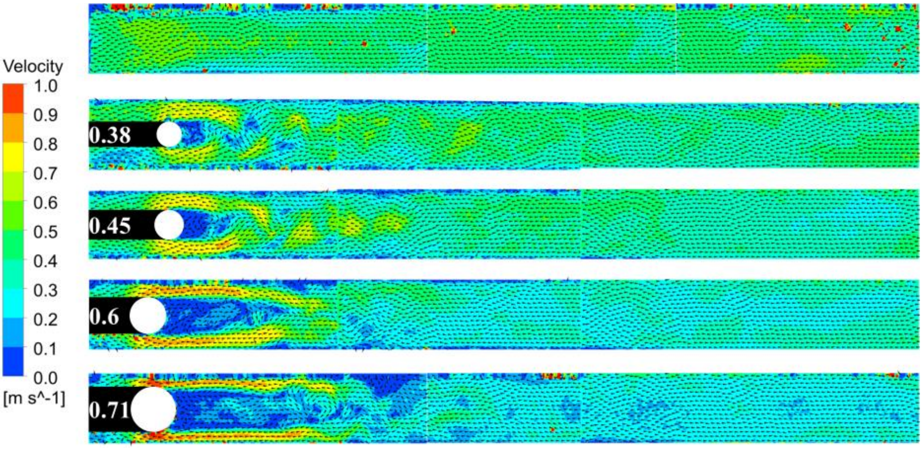

Figure 4: Instantanous velocity distribution (composed of three single instantanous sections)

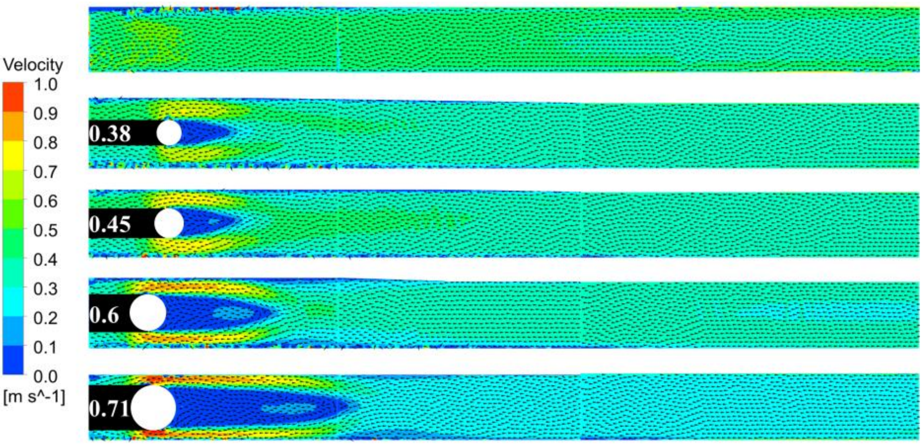

Figure 5: Averaged velocity distribution

By introducing a vortex promoting cylinder into the channel, the flow is modified significantly: the flow is accelerated when passing the cylinder and irregular counter-rotating vortices separate behind it, creating the Kármán vortex street. The enhanced mixing is confirmed. In all cylinder cases, vortex shedding is observed to be irregular and three-dimensional, although the channel geometry is two-dimensional (Figure 4).

With increasing blockage ratio, the velocity level in general decreases. This is due to the rising additional pressure drop of the cylinder. The irregular vortices develop further downstream the cylinder, resulting in a growing backflow region for growing blockage ratio (Figure 5). Compared to the reference case, the averaged velocity profile is more homogenous throughout the channel width.

4 Conclusions and Outlook

In this experimental study, heat transfer enhancement of free convection flows in heated 2D-channel is found to amount to up to 41.9% through triggering a vortex street by positioning a circular cylinder with a blockage ratio of 0.45 at a channel height of 25% in the flow. The HTE depends on the cylinder position as well as on the blockage ratio. The enhancement is achieved without adding any additional propelling energy, as the flow is purely driven by natural convection. The flow is found to be three-dimensional despite two-dimensional geometry.

The obtained PIV data is suitable for validation purposes of CFD calculations. However, further studies need to be done with multiple cylinder configurations and 3D channel geometries, different wall temperatures and different cylinder shapes.

Acknowledgment

Grateful acknowledgement is made to Rettig ICC for providing financial support.

References

[1] Abbassi, H., Turki, S., Nasrallah, S. Ben, 2002, "Numerical Investigation of Forced Convection in a Horizontal Channel With a Built-In Triangular Prism", J. Heat Transfer, 124 (3), p. 571.

[2] Biswas, G., Laschefski, H., Mitra, N. K., Fiebig, M., 1990, "Numerical Investigation of Mixed Convection Heat Transfer in a Horizontal Channel with a Built-in Square Cylinder", Numerical Heat Transfer, Part A: Applications, 18 (2), pp. 173–188.

[3] Ginnings, D.C., Furukawa G.T., 1953, “Heat Capacity Standards for the Range 14 to 1200 K”, Journal of the American Chemical Society, pp. 522-527.

[4] Harlow, F. H., Fromm, J. E., 1964, "Dynamics and Heat Transfer in the von Kármán Wake of a Rectangular Cylinder", Phys. Fluids, **7** (8), p. 1147.

[5] Hucho, W.-H., 2011, Aerodynamik der stumpfen Körper, Vieweg + Teubner, Wiesbaden.

[6] Icoz, T., Jaluria, Y., 2006, "Design Optimization of Size and Geometry of Vortex Promoter in a Two-Dimensional Channel", J. Heat Transfer, 128 (10), p. 1081.

[7] Mathis, P., Herpers, M., Müller, D., 2014, "Heat transfer enhancement in channels with natural convection flow by Kármán vortex streets", FEDSM2014-21076

[8] Meis, M., Varas, F., Velázquez, A., Vega, J. M., 2010, "Heat transfer enhancement in micro-channels caused by vortex promoters", International Journal of Heat and Mass Transfer, 53 (1-3), pp. 29–40.

[9] Oosthuizen, P. H., 2012, "Mixed Natural and Forced Convective Heat Transfer from a Horizontal Array of High Aspect Ratio Heated Isothermal Cylinders Placed in a Vertical Forced Flow", Proceedings of the Conference of the CFD Society of Canada, CFD2012, Canmore, Alberta, Canada.

[10] Persoons, T., O’Gorman, I. M., Donoghue, D. B., Byrne, G., Murray, D. B., 2011, "Natural convection heat transfer and fluid dynamics for a pair of vertically aligned isothermal horizontal cylinders", International Journal of Heat and Mass Transfer.

[11] Rosales, J. L., Ortega, A., Humphrey, J. A. C., 2000, "A Numerical Investigation of the Convective Heat Transfer in Unsteady Laminar Flow Past a Single and Tandem Pair of Square Cylinders in a Channel", Numerical Heat Transfer, Part A: Applications, 38 (5), pp. 443–465.
[12] Sarkar, S., Dalal, A., Biswas, G., 2010, "Mixed convective heat transfer from two identical square cylinders in cross flow at Re=100", International Journal of Heat and Mass Transfer, 53 (13-14), pp. 2628–2642.
[13] Singha, A. K., Sarkar, A., De, P. K., 2007, "Numerical Study on Heat Transfer and Fluid Flow Past a Circular Cylinder in the Vicinity of a Plane Wall", Numerical Heat Transfer, Part A: Applications, 53 (6), pp. 641–666.
[14] Stephan, P., 2013, VDI-Wärmeatlas, VDI e.V., VDI Verlag, Düsseldorf.
[15] Truckenbrodt, E., 2008, Fluidmechanik, Springer, Berlin, Heidelberg
[16] Wagner, W., Pruss, A., "The IAPWS formulation 1995 for the thermodynamic properties of ordinary water substance for general and scientific use", Journal of Physical and Chemical Reference Data, 2002, 31, 2, 387-535, [doi:10.1063/1.1461829].
[17] Raffel, M., Willert, C. E., Kompenhans, J. Particle Image Velocimetry: A Practical Guide, Springer, New York, 1998.
[18] Oleg G. Martynenko, Pavel P. Khramtsov. Free convective heat transfer, 2005, Springer, Berlin, Heidelberg.